Atomic-Scale Modeling of the Dynamics of Titanium Oxidation

Atomic-scale modelling of the dynamics of titanium oxidation

Linggang Zhu,[†,‡] Qing-Miao Hu,[*,‡] Rui Yang,[‡] and Graeme J. Ackland[*,†]

SUPA, School of Physics and Astronomy, The University of Edinburgh, Edinburgh EH9 3JZ, UK, and Shenyang National Laboratory for Materials Science, Institute of Metal Research, Chinese Academy of Sciences, Shenyang 110016, China

E-mail: qmhu@imr.ac.cn; gjackland@ed.ac.uk

[*]To whom correspondence should be addressed

[†]SUPA, School of Physics and Astronomy, The University of Edinburgh, Edinburgh EH9 3JZ, UK

[‡]Shenyang National Laboratory for Materials Science, Institute of Metal Research, Chinese Academy of Sciences, Shenyang 110016, China

Abstract

We present a model for the oxidation of titanium combining non-equilibrium statistical mechanics and Density Functional Theory (DFT). We find that oxygen is more strongly bound as an interstitial in Ti than in TiO_2 oxide, the energy difference being around 1.6 eV. Therefore, a binary phase structure TiO_2/Ti, like the commonly-observed oxide scale, which protects titanium alloy against corrosion, is thermodynamically unstable. Likewise, various DFT functionals all show several TiO_{2-x} compounds, have lower energy than the weighted average of Ti and TiO_2. Thus the scale is a non-equilibrium structure and diffusion is the controlling process. We find that the barrier for O-vacancy migration in TiO_2 is $E_{rutile} = 0.9$ eV, much lower than the interface migration barriers (1.0-1.9 eV). We introduce a particle-based diffusion model which captures this feature, and explains the long-lived nature of the observed thin oxide layer.

Due to low density, high strength, and excellent corrosion resistance, Ti and its alloys are widely used in many fields. However, above 600°C, the surface loses its corrosion protection due to continuous growth.[1] Improving oxidation resistance is essential to extend Ti-alloy use to high temperature, and a better understanding of the process of Ti oxidation will optimize the methods to design such alloys.

Experimentally, a rutile (TiO_2 tetragonal, *P4₂/mnm*) scale forms on oxidized titanium,[2–5] with a sharp boundary (see TOC image) of well defined crystallographic orientation relationship (COR).[2] By contrast, the Ti-O phase diagram[6] shows a series of solution/compounds forming at intermediate oxygen concentration, like Ti_2O (space group: $P\bar{3}m1$),[7] TiO (*C12/m1*, *low temperature structure*),[8] Ti_2O_3 ($R\bar{3}c$),[9] etc.. Other different stoichiometric and structures have been found in ultrathin TiO_x films.[10–12] These structures correspond to filling the interstices in a hexagonal Ti lattice, so although there is some tendency for the O interstitials to order in layers, the experimental phase diagram can be viewed as a solid solution for compositions from Ti to TiO_2.

Resolving the conflict between the observed sharp interface, and the thermodynamic prediction of continuous solid solution is the subject of this paper.

Atomic-level investigation of oxidation is experimentally difficult, and so theoretical study, using DFT, has become the method of choice to obtain a detailed understanding. Previous work

showed that the change in chemical bonding from ionic to metallic is extremely abrupt, occurring across a few Angstroms at the interface.[13] Further, the Ti-TiO_2 interface has a negative formation energy, consistent with the continuous solid solution inferred from the phase diagram. However the dynamics of atomic migration have not been reported, and are examined here by DFT.

The most commonly observed, near-epitaxial Ti$(10\bar{1}0)$[0001] // $TiO_2(100)$[010] interface,[13] allows numerous different stackings, with the oxide terminated with either a single-oxygen interface (one layer of oxygen on the interface, i.e., the TiO_2 part is terminated with O-Ti-O) or a double-oxygen interface (two layers of oxygen on the interface). Both must be present as oxidation proceeds. This gives rise to many possible transition paths, so here, we concentrate on oxygen diffusion from the most stable structures in these two categories. Our calculations use supercells containing metal and oxide regions.

To calculate the energetics of oxidation, we removed one oxygen atom from the interface (or from the oxide), creating a vacancy, and replace it in interstitial site in the metal. Surprisingly, in all cases, this lowers the total energy (Figure 2), by 1.6eV (O from bulk); 1.0eV (O from single-oxygen interface); or 0.6eV (double-oxygen interface). These energies converge quickly as the oxygen interstitial is moved deeper into the bulk metal, due to effective metallic screening.

Further investigation shows that, the system consisting of Ti, TiO_2 and a sharp interface, is energetically unfavourable compared to having oxygen mixed homogeneously. Indeed, the Ti-O phase diagram,[6] shows various stable compounds (Ti_2O, TiO) with sub-stoichiometric oxygen concentrations. Figure 1 shows that the calculated energies of several TiO_{2-x} compounds agrees with the phase diagram. For example, for the ordered compound TiO, the energy of one TiO unit is 0.5-0.6 eV lower than the average of the Ti and TiO_2. As seen from Figure 1, when the ratio of oxygen and titanium is between 0 and 2, Ti-O solution or other compounds are more stable than the binary system TiO_2/Ti.

Thus our static DFT calculations agree with the experimental Ti-O phase diagram[6] which is consistent with the interface result that the total energy drops when one oxygen in the oxide moved to the interstice of the Ti. Therefore, with composition TiO_{2-x}, TiO_2+Ti is not the most stable

arrangement, and should not be formed at equilibrium.

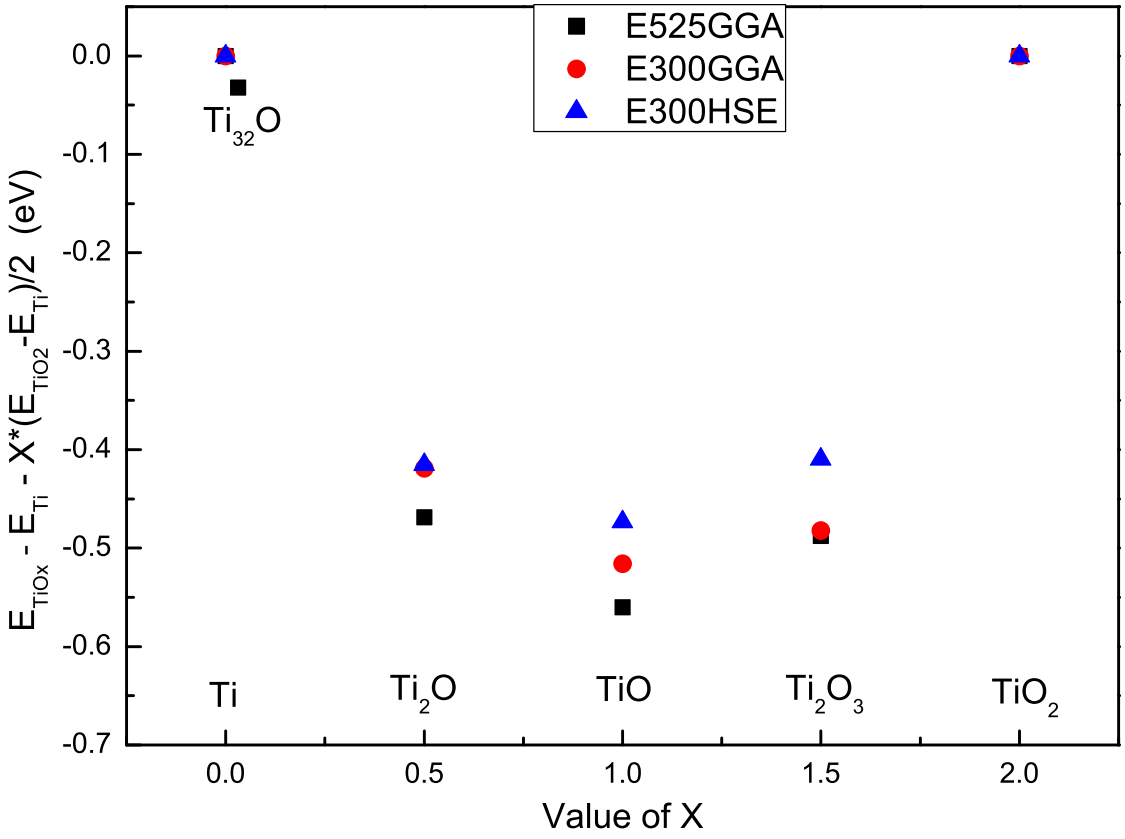

Figure 1: Energy of the Ti-O systems. Black squares are obtained using 525 eV plane wave cutoff and PW91-GGA. Red circles used 300 eV and PW91-GGA. Blue triangles used HSE06 with 300 eV cutoff. $Ti_{32}O$ has one octahedral oxygen interstitial in a 32-atom Ti supercell. Other phases taken from Massalski.[6] Further details under 'Calculational Methods'.

Both the Ti-O phase diagram and our calculation above suggest that the bulk Ti with thin TiO_2 layer on top is actually a thermodynamically unstable system. However, experiments invariably observe rutile on top of Ti, and oxygen seems unable to go deeply into the metal. To explain this, data about the diffusion process of oxygen in the oxide/metal system is needed.

The energy barrier for O-diffusion from the interface into the metal was calculated using Climb Image-Nudged Elastic Band (CI-NEB) method.[14,15] The energy profile and transition state structures are shown (Figure 2). The energy barrier depends on the interface structure: for the single-oxygen interface the barrier $E_{BOIS} = 1.9eV$ and for the double-oxygen one the barrier $E_{BOID} = 1.0eV$. This is in reasonable agreement with the measured barrier 1.5 eV for the dif-

fusion of oxygen across the interface between amorphous TiO_2 and Ti.[16]

Natural rutile is usually reduced, i.e., TiO_{2-x} (0 <x <2), so oxygen vacancies or titanium interstitial occur naturally. Consequently, we used a $2 \times 2 \times 3$ supercell with k-point mesh $3 \times 3 \times 3$ to study the diffusion of oxygen via vacancy mechanism in TiO_2. There are three inequivalent pathways, which are shown in the unit cell in Figure 3 and denoted as 'A', 'B' and 'C'. CI-NEB calculation showed that the energy barrier for these three pathways are 1.2 eV, 0.9 eV, and 2.1 eV, respectively. Diffusion pathway 'C' has no component in the direction [100], so cannot contribute to the diffusion in this direction. Both 'A' and 'B' contribute to the diffusion across the interface studied here. Iddir et.al.[17] reported the migration barrier for a charged oxygen vacancy (V_o^{2+}) is 1.1 eV, 0.69 eV, and 1.77 eV, for path 'A', 'B' and 'C', respectively. Thus, the neutral and the charged oxygen vacancy share the easier diffusion pathway ('A' and 'B'). We assume that there is a smaller barrier for the charged ion because fewer electrons leave a larger 'space' for diffusion.

The diffusion barrier of oxygen in bulk Ti is around 2 eV, with similar values for various diffusion paths. This agrees with previous work performed by Wu et.al..[18] Based on the low diffusion barrier in rutile (TiO_2) and high value in Ti and across the interface, we conclude that the growth of the scale in the oxidation is be controlled by the diffusion of oxygen into the titanium matrix.

In principle, the outward movement of titanium may also contribute to the oxidation. We calculated the energy change when Ti atoms on the interface (or in the center of the metal) moved into the interstices of the oxide (Table 1). This shows that it is favourable for interfacial Ti to go into the oxide, but overall movement from the center of the metal increases the system energy. Thus the diffusion of oxygen vacancies is the dominant process in oxidation.

The picture which emerges from the calculations above is as follows. When the oxidation starts, oxygen can easily dissolve in the surface of the Ti, but it is trapped there by the high barrier against diffusion into the metal. As the interface moves slowly against this barrier, there is plenty of time for further oxygen to arrive from the surface to saturate the oxide at the TiO_2 composition. Thus, the formation of TiO_2 becomes possible, despite the thermodynamics. Since oxygen beyond the

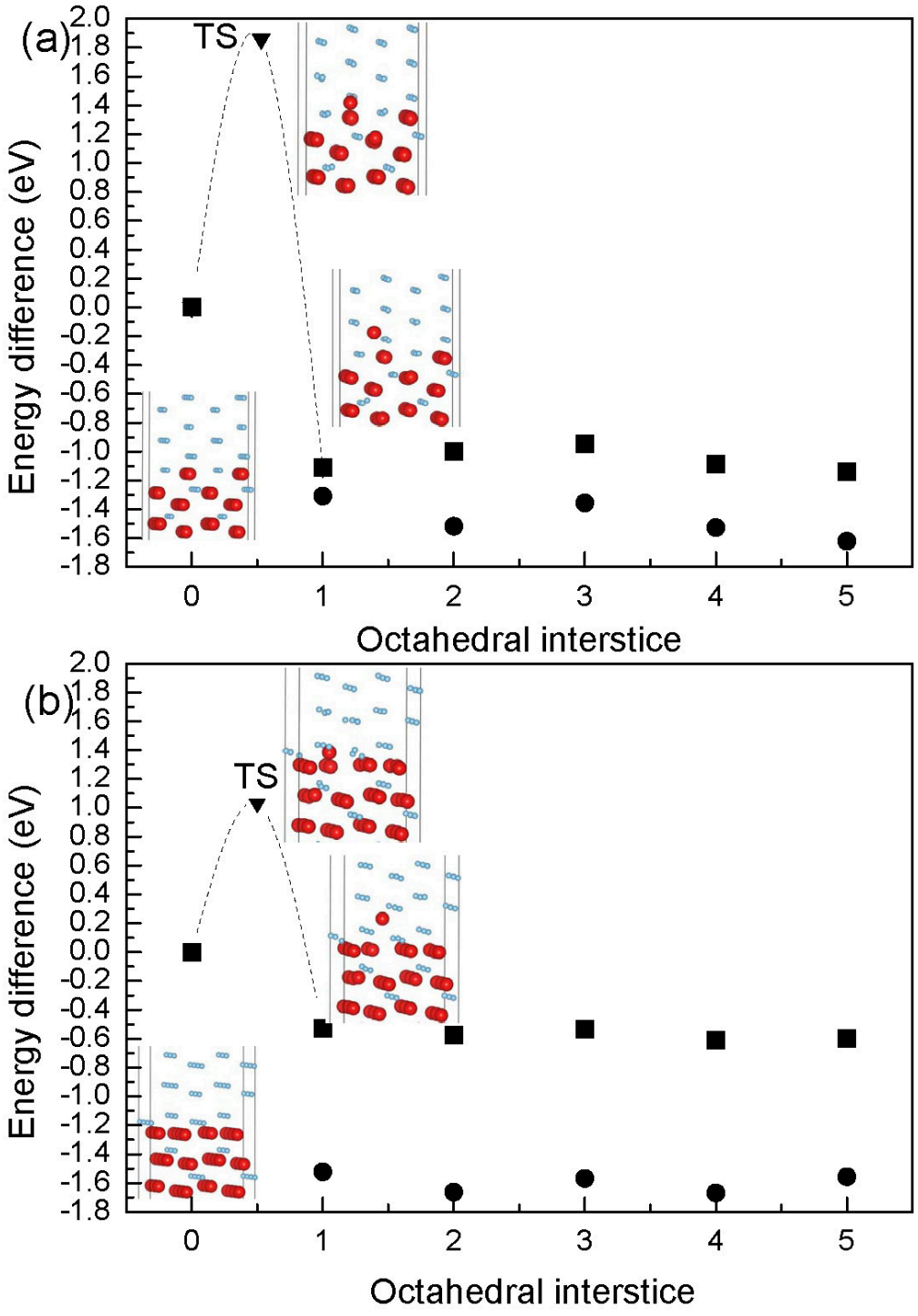

Figure 2: Energy variation when one oxygen atom is relocated to an octahedral interstice in layer X of the metal leaving a vacancy in the interface (squares) or bulk (circle). X=0 corresponds to perfect interface structure. The dashed line is the CI-NEB energy profile for oxygen hopping from interface to metal. The (partial) atomic structures of the perfect interface, transition states (TS), and that with oxygen in the nearest octahedral interstice are shown for (a) single-oxygen interface, (b) double-oxygen interface. Red (silver) balls represent oxygen (titanium) atoms.

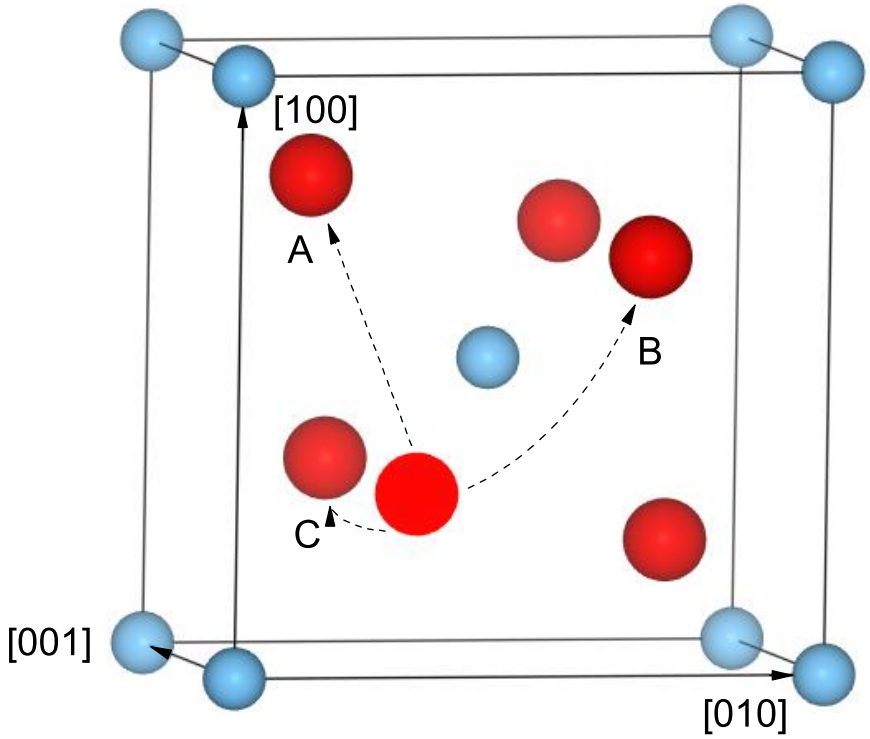

Figure 3: Diffusion path of neutral oxygen vacancy in rutile. Red balls are oxygen, unshaded red circle is the vacancy site. Blue balls are titanium.

Table 1: Energy of the interface containing defects compared with perfect interface structure. $I_v + C_i$ means structures with one Ti vacancy on the interface and one interstitial Ti in the center of the oxide, while $C_v + C_i$ represents one Ti vacancy in the center of the metal and one interstitial Ti in the center of the oxide. Ti interstitials have several inequivalent positions with respect to the TiO_2, and the energy scatter is shown below.

	single-oxygen interface	double-oxygen interface
$I_v + C_i$	-1.0/-1.2	-0.5/-0.6
$C_v + C_i$	+0.0/+0.2	+0.2/+0.3

TiO_2/Ti interface can move within the metal by overcoming a relatively smaller barrier, a diffuse, but oxygen rich region exists under the scale. This region is narrow at relatively low temperature, but when the temperature rises, oxygen diffuses faster in the metal, and the system moves towards thermodynamic equilibrium, stable vacancy defects are produced, the more porous oxide layer grows faster and corrosion resistance is lost.

As the dissolution energy of oxygen in Ti is very high, and heat conduction in Ti is poor, a large amount of heat might be generated during oxidation, which in then causes still faster oxidation. Since no protective scale can be formed, if sufficient temperature can be reached, the high-temperature reaction becomes self-sustaining and the titanium burns.

We have shown that oxidation must be regarded as a non-equilibrium process, and we now cast the preceding verbal argument into a precise model.

The large barrier for lateral motion, process 'C' in Figure 3, suggests considering diffusion as a 1D process. An appropriate simple non-equilibrium model is the 1D hopping model with extension, shown in Figure 4. This model considers a line of 'oxide' sites which may be occupied by an oxygen atom (state 1), or not (state 0). An oxygen atom can hop from one site to an adjacent open site. One end represents the free surface, where oxygen is supplied but not removed, the other end represents the TiO_2/Ti interface, where movement of an oxygen extends the oxide region, and hence the length of the line.

This is based on a model well-known in statistical physics, the symmetric simple exclusion process. The novel feature of line-extension has not been solved to our knowledge, although a similar extending process has been solved for the asymmetric exclusion process applied to fungal growth[19] and our simulations show similar behaviour, a slowly extending jammed phase for high β/γ (the oxide scale) (see Figure 4 for definition) and a free flowing phase for $\beta/\gamma < 1$.

The behavior of this model depends on the ratios between α, β and γ. It is reasonable to assume a high value of α: that surface vacancies are quickly filled. In fact only this regime can produce a surface oxide layer. At high $\beta/\gamma = exp(-E_{rutile} + E_{BOIS}/kT)$ the system can be analytically solved: it jams. Our simulations of this system confirm its equivalence to the fungal model; in

the mean field solution the oxide has the surface site occupied, the interface site occupied with probability $1-\gamma/\beta$, and a linear profile between.[19]

In this regime, appropriate for describing the scale, the growth rate decreases sharply with layer thickness L, being proportional to the rate of producing O vacancies ($\gamma \propto \exp(-E_{BOIS}/kT)$ at the interface times the probability that the vacancy will diffuse to the surface rather than returning to the interface $(1/L)$. The first term is constant, at given temperature, the second is essentially temperature independent. External temperature increase reduces β/γ, meaning increased oxidation rate, but cannot reach $\beta/\gamma < 1$ which would correspond to a dynamical phase transition where the oxide collapses (more vacancies than atoms). This transition is equivalent to burning, and could be achieved when the energy release at the interface leads to a higher temperature there than in the environment.

This hopping model gives a direct connection to the calculated barrier heights, and is more easily applied than, e.g., the Deal-Grove[20] diffusion model which is more applicable to interstitial mediated diffusion, but even there has been strongly criticized.[21] Our model predicts a squart root relationship between thickness and time at low temperature, switching to faster growth when the O vacancies are no longer independent. This is consistent with data from Kofstad et.al..[22]

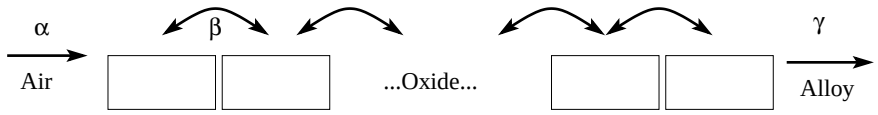

Figure 4: Hopping model for Ti oxidation. α is the absorption rate, taken as 1, β the barrier crossing rate in the oxide, dependent on the barrier E_{rutile} and γ the interface crossing rate, dominated by the barrier for oxygen migration in the interface with single O-layer E_{BOIS} and in the Ti matrix. When the interface is crossed, the length of oxide extends, if the final site is empty, it retreats.

In summary, our DFT calculation showed that the normally observed system: a thin TiO_2 layer on bulk Ti, is thermodynamically unstable, and the more stable state involves oxygen penetrating into the bulk. The outward diffusion of oxygen vacancies is the key mechanism in TiO_2. However, migration of oxygen is kinetically blocked by the high diffusion barriers to bulk Ti, and this is the controlling process in oxidation. Oxygen moves more easily from the surface when partial oxidation has occurred, and this leads to saturation and formation of TiO_2.

We map this process onto a hopping diffusion model with extension. This model shows that the non-equilibrium diffusion process does lead to a sharp phase boundary between oxide and metal. Furthermore it correctly predicts that the oxide growth rate becomes significantly slower as the thickness increases, but shows Arrhenius behavior with temperature.

From this model, we deduce that burning will arise when the rate of oxygen-hopping into the metal becomes higher than in rutile. Although the barrier is always higher, the release of energy at the interface means that the local temperature is always higher. The controlling parameter for the rate is E/T, and at $\beta/\gamma = 1$ the hopping model exhibits a dynamical phase transition to free-flowing oxygen: burning.

Calculational Methods

All calculations are performed using the Vienna Ab initio Simulation Package (VASP).[23–25] The electronic exchange-correlation interactions are described by generalized gradient approximation (GGA) parameterized by Perdew and Wang (PW91).[26] The 3p3d4s and 2s2p electrons are treated explicitly for Ti and O: our systems containing up to 3000 electrons. $3 \times 2 \times 1$ supercells were used, and the dimensions on the interface plane are 8.9 Å$\times$ 9.1 Å, which is large enough to eliminate interaction between defects (interstitial atom or vacancy) and their images. For the interface structure calculation, we use Γ k-point sampling. The cutoff energy is set as 300 eV. Structural optimizations use fixed supercells, with atomic forces relaxed to below 0.05 eV/Å. The metal is slightly expanded to achieve epitaxy, but we found this has negligible effects on the defect energies.

For the bulk Ti-O solution/compound, we used two sets of k-point sampling. With cutoff energy 525 eV, for Ti, Ti_2O, TiO, Ti_2O_3, and TiO_2, k-point mesh are $11 \times 11 \times 7$, $11 \times 11 \times 7$, $7 \times 7 \times 5$, $7 \times 7 \times 7$, and $5 \times 5 \times 8$, respectively. To be consistent with the interface structure calculation, we recalculate the energy with cutoff energy 300 eV. To use the hybride functional HSE06,[27] coarser k-point meshes were needed. They are $3 \times 3 \times 2$, $3 \times 3 \times 2$, $2 \times 2 \times 2$, $3 \times 3 \times 3$, and $3 \times 3 \times 5$. During these simulations, both cell shape and position of atoms are relaxed to forces smaller than

0.01 eV/Å.

The Bader charge[28] of oxygen is -1.10e in the centre of the oxide, but increases to -1.44e for the oxygen in the interstice of the metal. This may account for the stability of the 'defective' system compared to the perfect interface structure.

A common dilemma in studying diffusion in oxides is whether the defect should be charged. This is not a problem in our calculations, since the presence of the metal in the supercell enables the oxygen ions to change its charge state at will, always adopting the lowest energy state. The exchange correlation functional can have major effects on TiO_2.[29] Problems may occur with soft modes and the band gap, so we cross-check our results with the hybrid functional HSE06[27] in addition to the standard exchange-correlation functional GGA.[26] HSE06 gives a band gap of 2.7 eV, close to previous work,[30] and the experimental value 3.0 eV.[31]

All our conclusions are independent of the exchange-correlation functional, although it is notable that a higher cutoff is required to converge the energy of the lower symmetry Ti_2O and TiO structures than the pure Ti and TiO_2. This is probably on account of the polarization of the oxygen ion, which is only fully described by including the higher energy plane waves.

Acknowledgement

The authors would like to acknowledge the support of the European Union Seventh Framework Programme (FP7/2007-2013) under grant agreement No. PITN-GA-2008-211536, project MaMiNa. The authors also acknowledge the financial support from the MoST of China under Grant No. 2011CB606404. The SEM picture of oxidized Ti in the TOC is kindly provided by Carsten Siemers, and the picture of the burning Ti is from NASA. We thank Bengt Tegner, Martin Evans and Richard Blythe for useful discussions.

References

(1) Lutjering, J. C., G.and Williams, Ed. *Titanium*, 2nd ed.; Springer: Germany, 2007.

(2) Flower, H.; Swann, P. An in situ study of titanium oxidation by high voltage electron microscopy. *Acta Metall.* **1974**, *22*, 1339 – 1347.

(3) Kozlowski, M.; Tyler, P.; Smyrl, W.; Atanasoski, R. Photoelectrochemical microscopy of oxide films on metals: Ti/TiO2 interface. *Surf. Sci.* **1988**, *194*, 505 – 530.

(4) Ting, C.-C.; Chen, S.-Y.; Liu, D.-M. Preferential growth of thin rutile TiO2 films upon thermal oxidation of sputtered Ti films. *Thin Solid Films* **2002**, *402*, 290 – 295.

(5) Kumar, S.; Narayanan, T. S.; Raman, S. G. S.; Seshadri, S. Thermal oxidation of CP Ti-An electrochemical and structural characterization. *Mater. Charact.* **2010**, *61*, 589 – 597.

(6) Massalski, H., T.B.and Okamoto, Subramanian, P., Kacprzak, L., Eds. *Binary Alloy Phase Diagrams*, 2nd ed.; ASM International: US, 1990; online phase diagram: http://www1.asminternational.org/asmenterprise/APD/.

(7) Kornilov, I.; Vavilova, V.; Fykin, L.; Ozerov, R.; Solowiev, S.; Smirnov, V. Neutron diffraction investigation of ordered structures in the titanium-oxygen system. *Metall. Mater. Trans. B* **1970**, *1*, 2569–2571.

(8) Watanabé, D.; Castles, J. R.; Jostsons, A.; Malin, A. S. The ordered structure of TiO. *Acta Crystallogr.* **1967**, *23*, 307–313.

(9) Rice, C. E.; Robinson, W. R. High-temperature crystal chemistry of Ti_2O_3: structural changes accompanying the semiconductor–metal transition. *Acta Crystallogr., Sect. B* **1977**, *33*, 1342–1348.

(10) Wu, C.; Marshall, M. S. J.; Castell, M. R. Surface Structures of Ultrathin TiOx Films on Au(111). *J. Phys. Chem. C* **2011**, *115*, 8643–8652.

(11) Barcaro, G.; Cavaliere, E.; Artiglia, L.; Sementa, L.; Gavioli, L.; Granozzi, G.; Fortunelli, A. Building Principles and Structural Motifs in TiOx Ultrathin Films on a (111) Substrate. *J. Phys. Chem. C* **2012**, *116*, 13302–13306.

(12) Ohwada, M.; Kimoto, K.; Suenaga, K.; Sato, Y.; Ebina, Y.; Sasaki, T. Synthesis and Atomic Characterization of a Ti2O3 Nanosheet. *J. Phys. Chem. Lett.* **2011**, *2*, 1820–1823.

(13) Zhu, L.; Hu, Q.-M.; Yang, R.; Ackland, G. J. Binding of an Oxide Layer to a Metal: The Case of Ti(101(bar)0)/TiO2(100). *J. Phys. Chem. C* **2012**, *116*, 4224–4233.

(14) Henkelman, G.; Uberuaga, B. P.; Jónsson, H. A climbing image nudged elastic band method for finding saddle points and minimum energy paths. *J. Chem. Phys.* **2000**, *113*, 9901–9904.

(15) Sheppard, D.; Terrell, R.; Henkelman, G. Optimization methods for finding minimum energy paths. *J. Chem. Phys.* **2008**, *128*, 134106–134115.

(16) Zalar, A.; van Lier, J.; Mittemeijer, E.; Kovac, J. Interdiffusion at TiO2/Ti, TiO2/Ti3Al and TiO2/TiAl interfaces studied in bilayer structures. *Surf. Interface Anal.* **2002**, *34*, 514–518.

(17) Iddir, H.; Öğüt, S.; Zapol, P.; Browning, N. D. Diffusion mechanisms of native point defects in rutile TiO_2: *Ab initio* total-energy calculations. *Phys. Rev. B* **2007**, *75*, 073203–073206.

(18) Wu, H. H.; Trinkle, D. R. Direct Diffusion through Interpenetrating Networks: Oxygen in Titanium. *Phys. Rev. Lett.* **2011**, *107*, 045504–045507.

(19) Sugden, K. E. P.; Evans, M. R. A dynamically extending exclusion process. *J. Stat. Mech.* **2007**, *2007*, P11013–P11032.

(20) Deal, B. E.; Grove, A. S. General Relationship for the Thermal Oxidation of Silicon. *J. Appl. Phys.* **1965**, *36*, 3770–3778.

(21) Stoneham, A. M.; Gavartin, J. L.; Shluger, A. L. The oxide gate dielectric: do we know all we should? *J. Phys.: Condens. Matter* **2005**, *17*, S2027–S2049.

(22) Kofstad, P.; Hauffe, K.; Kjollesdal, H. Investigation of the oxidtion mechanism of titanium. *Acta Chem. Scand.* **1958**, *12*, 239–266.

(23) Kresse, G.; Hafner, J. *Ab initio* molecular dynamics for liquid metals. *Phys. Rev. B* **1993**, *47*, 558–561.

(24) Kresse, G.; Furthmüller, J. Efficient iterative schemes for *ab initio* total-energy calculations using a plane-wave basis set. *Phys. Rev. B* **1996**, *54*, 11169–11186.

(25) Kresse, G.; Furthmuller, J. Efficiency of ab-initio total energy calculations for metals and semiconductors using a plane-wave basis set. *Comput. Mater. Sci.* **1996**, *6*, 15–50.

(26) Perdew, J. P.; Wang, Y. Pair-distribution function and its coupling-constant average for the spin-polarized electron gas. *Phys. Rev. B* **1992**, *46*, 12947–12954.

(27) Paier, J.; Marsman, M.; Hummer, K.; Kresse, G.; Gerber, I. C.; Ángyán, J. G. Screened hybrid density functionals applied to solids. *J. Chem. Phys.* **2006**, *124*, 154709–154721.

(28) Tang, W.; Sanville, E.; Henkelman, G. A grid-based Bader analysis algorithm without lattice bias. *J. Phys.: Condens. Matter* **2009**, *21*, 084204–084210.

(29) Refson, K.; Montanari, B.; Mitev, P.; Hermansson, K.; Harrison, N. Comment on "First-principles study of the influence of (110)-oriented strain on the ferroelectric properties of rutile TiO2". **2012**, Submitted.

(30) Lu, Y. H.; Xu, B.; Zhang, A. H.; Yang, M.; Feng, Y. P. Hexagonal TiO2 for Photoelectrochemical Applications. *J. Phys. Chem. C* **2011**, *115*, 18042–18045.

(31) Grant, F. A. Properties of Rutile (Titanium Dioxide). *Rev. Mod. Phys.* **1959**, *31*, 646–674.

Graphical TOC Entry